JOURNAL OF VIROLOGY, Jan. 2003, p. 631–641 Vol. 77, No. 1
0022-538X/03/$08.00+0 DOI: 10.1128/JVI.77.1.631–641.2003

Disruption of Mitochondrial Networks by the Human Cytomegalovirus *UL37* Gene Product Viral Mitochondrion-Localized Inhibitor of Apoptosis

A. Louise McCormick, Vanessa L. Smith, Dar Chow, and Edward S. Mocarski*

Department of Microbiology and Immunology, Stanford University School of Medicine, Stanford, California 94305-5124

Received 17 June 2002/Accepted 26 September 2002

By 24 h after infection with human cytomegalovirus, the reticular mitochondrial network characteristic of uninfected fibroblasts was disrupted as mitochondria became punctate and dispersed. These alterations were associated with expression of the immediate-early (α) antiapoptotic *UL37x1* gene product viral mitochondrion-localized inhibitor of apoptosis (vMIA). Similar alterations in mitochondrial morphology were induced directly by vMIA in transfected cells. A 68-amino-acid antiapoptotic derivative of vMIA containing the mitochondrial localization and antiapoptotic domains also induced disruption, whereas a mutant lacking the antiapoptotic domain failed to cause disruption. These data suggest that the fission and/or fusion process that normally controls mitochondrial networks is altered by vMIA. Mitochondrial fission has been implicated in the induction of apoptosis and vMIA-mediated inhibition of apoptosis may occur subsequent to this event.

Human cytomegalovirus (CMV), a betaherpesvirus, is a large DNA virus whose genome contains more than 200 open reading frames, some of whose products are committed to blocking apoptosis (30). Like other large DNA viruses, CMV may alter the cell in ways that induce apoptosis. Adenoviruses, iridoviruses, poxviruses, and herpesviruses encode functions that induce as well as prevent host cell death, and some of these localize to mitochondria. Antiapoptotic properties have been reported for several viral immediate-early (α) gene products (*UL122*, *UL123*, *UL36*, and *UL37*) (19, 20, 38, 40, 47, 49), but mechanisms of action are only understood for *UL36* and *UL37* (19, 20, 38). The smallest *UL37* gene product, pUL37x1, encodes a potent antiapoptotic function called viral mitochondrion-localized inhibitor of apoptosis (vMIA) (20). The activity of vMIA, which is also conserved in two larger glycoproteins encoded by *UL37*, gpUL37, and gpUL37$_M$, prevents release of cytochrome *c* from mitochondria. vMIA may function via an association with an adenine nucleotide translocator (ANT) (19, 20), a component of the mitochondrial membrane permeability transition pore complex (5). All three *UL37* gene products are cytoplasmic proteins that traffic through the secretory pathway to mitochondria (8). While the activities of the two larger *UL37* gene products may extend to regulation of gene expression (23), *UL37x1* function is focused on blocking apoptosis (20, 22).

Viral infection may induce apoptosis via mitochondrial events due to cell stress or DNA damage, such as has been well established for adenoviruses (12, 45). Intrinsic apoptosis may also occur during CMV infection, and cell survival may require the action of viral antiapoptotic functions. Transcriptional regulatory proteins such as adenovirus E1A are proapoptotic and require an antiapoptotic function such as E1B for cell survival. Apoptosis during CMV infection may result from the cell cycle block by virion proteins such as ppUL69 (28) or α gene products such as the 579-amino-acid IE2-p86 (IE2$_{579aa}$) (32). Virus-infected cells are also subjected to host immune clearance mechanisms that lead to apoptosis. Mammalian hosts employ apoptosis as a means of immune control via death receptors in the tumor necrosis factor (TNF) family including Fas, TNF-alpha receptor, and TNF-alpha-related apoptosis-inducing ligand receptor (2, 44). Additional control includes cell-mediated killing of virus-infected cells by the innate, natural killer (NK) or adaptive, cytotoxic-T-cell immune responses (14). A major, evolutionarily conserved consequence of these immune effectors is the induction of apoptosis, and a wide variety of viruses, including CMV, have evolved ways of overcoming cell death.

Although functionally similar to antiapoptotic Bcl-2 family proteins, vMIA lacks Bcl-2 homology domains, shares no obvious amino acid sequence homology with Bcl-2 family members, and does not appear to interact with the voltage-dependent anion channel (19, 20, 43). vMIA is one of the most potent inhibitors of mitochondrion-mediated cell death and confers resistance to apoptosis induced by stress, DNA damage, death receptor signaling, reactive oxygen species, and respiration poisons (3, 24, 43). vMIA has two domains that are required for function. The first domain, overlapping with the signal sequence, targets vMIA to mitochondria and is located between amino acids 5 and 34 (22). The second domain necessary for preventing apoptosis is located between amino acids 118 and 147 (22). A 68-amino-acid minimal derivative of vMIA consisting of these two domains is fully functional. vMIA is conserved in all human CMV strains as well as in other primate CMVs that have been examined (19, 20). Laboratory strains of CMV that have been cultured for a prolonged period have accumulated mutations that disrupt expression of pUL36 and both gpUL37 and gpUL37$_M$. Of the characterized *UL36* and *UL37* gene products, AD169*var*ATCC encodes vMIA/pUL37x1, gpUL37, and gpUL37$_M$ but does not encode a func-

* Corresponding author. Mailing address: Department of Microbiology & Immunology, Fairchild Science Building, Stanford University School of Medicine, Stanford, CA 94305-5124. Phone: (650) 723-6435. Fax: (650) 723-1606. E-mail: mocarski@stanford.edu.

tional pUL36 (20, 38). Towne*var*RIT3 expresses vMIA but no other *UL36 or UL37* gene products (20, 38). It appears from analysis of these spontaneous mutants as well as from the construction of deletion mutants (4, 35) that vMIA may be the only product encoded in this region that is essential for replication in cultured human fibroblasts (HFs).

Mitochondria can exist in a cell as interconnected 0.5-μm-diameter tubular networks that appear as a reticulum or as multiple individual punctate organelles (46). Reticular mitochondria may undergo fission (the conversion to a punctate pattern) and fusion (the reverse process). Conversion from one form to the other occurs in response to changes in aerobic energy requirements or cell cycle and results in an altered cytosolic Ca^{2+} response (10). Fibroblasts generally exhibit a reticular pattern, although mitochondria change in shape as cells divide. The reticular pattern normally observed in COS-7 cells becomes disrupted and appears punctate during mitochondrion-dependent apoptosis (16). Redistribution of mitochondria has also been observed during death receptor-induced apoptosis of lymphoblastoid cells (13, 27). A dominant negative mutant of the mitochondrial fission protein, dynamin-related protein 1, inhibits mitochondrion-mediated apoptosis as well as mitochondrial fission (16). In addition, mitochondrial patterns vary with a wide variety of physiological and pathological states, some associated with viral disease. CMV stimulates mitochondrial DNA synthesis (17), as well as lipid turnover (26). The relevance of these alterations to viral infection is not yet understood.

Here we have sought to investigate the effects of vMIA on reticular mitochondria in CMV-infected and vMIA-expressing cells. We find that disruption of mitochondria may be a component of vMIA-mediated inhibition of apoptosis.

MATERIALS AND METHODS

Cells and viruses. Primary HFs were maintained in Dulbecco's modified Eagle medium (Gibco/BRL, Grand Island, N.Y.) including 10% NuSerum (Invitrogen, Carlsbad, Calif.), penicillin G (100 U/ml), streptomycin sulfate (100 mg/ml), L-arginine (0.58 mg/ml), L-glutamine (1.08 mg/ml), and L-asparagine (180 mg/ml). HeLa cells (from Karla Kirkegaard) were maintained in the same medium. For some experiments, culture medium also included antibody 7C11 at 0.2 μg/ml (Coulter, Fullerton, Calif.) and cycloheximide (CH) at 10 μg/ml (Sigma, St. Louis, Mo.). Sf9 cells (from Chris Garcia) were maintained in SF-900 medium (Gibco/BRL) supplemented with L-glutamine, 10% fetal calf serum (Gemini BioProducts, Woodland, Calif.), and gentamicin at 0.5 μg/ml (Gibco/BRL). Human CMV strains AD169*var*ATCC, obtained from the American Type Culture Collection, and Towne*var*RIT3, a subclone of Towne (vaccine lot 131 from Recherches et Industries Therapeutiques [now SmithKline Beecham Biologicals]) obtained from S. Plotkin (in 1992). For inhibition of viral α gene expression, culture medium included CH (50 μg/ml). The transient transfection reagent SuperFect (Qiagen, Valencia, Calif.) was used to introduce plasmid pcDNA3UL37x1myc (20) or pEGFP-puro (1) according to the manufacturer's instructions for transfection of mammalian cells. Sf9 cells were transfected using CellFectin (Invitrogen) according to the manufacturer's protocol.

Antibodies. Monoclonal mouse antibodies to Fas, 7C11 (Coulter); to CMV IE1 and IE2 proteins, MAb810 (Chemicon, Temecula, Calif.); to mitochondrial heat shock protein 70 (mtHSP70) (a gift from Susan Pierce, Northwestern University); and to a c-myc epitope, 9E10 (Santa Cruz Biotechnology, Santa Cruz, Calif.), were used. Polyclonal rabbit antiserum 313 to pUL37x1 was a gift from Victor Goldmacher (Immunogen, Inc., Cambridge, Mass.). Secondary antibodies were fluorescein- or Texas Red-conjugated horse anti-mouse immunoglobulin G (Vector, Burlingame, Calif.).

MitoTrackerRed stain and evaluation of mitochondrial morphology. MitoTrackerRed CMXRos (Molecular Probes, Eugene, Oreg.) was added to culture medium at a final concentration of 20 ng/ml and applied to HFs for 30 min at 37°C. This medium was removed, cells were washed with phosphate-buffered saline (PBS), and culture medium was added. Following a 2-h incubation period at 37°C, cells were treated with 3.7% formaldehyde (Sigma) and visualized by epifluorescence microscopy. To determine mitochondrial patterns in transient and stable cell cultures, a minimum of 200 cells were examined. For temporal analysis following transient expression, the mean and standard deviation was determined from 700 (12 h posttransfection), 550 (24 h posttransfection), or 350 (48 h posttransfection) vMIA-positive cells, and assessment of mitochondrial patterns was performed in a blinded manner (i.e., encoded slides were assessed in random order). This survey was performed on images collected through a 100× oil immersion objective with a Hamamatsu Orca-100 digital camera and Image Pro Plus software (MediaCybernetics).

Immunofluorescence assay. Cells grown on coverslips were fixed by addition of 3.7% formaldehyde and permeabilized by treatment with 0.5% Triton X-100 (Baker, Phillipsberg, Pa.) in PBS. After blocking with 5% horse serum (Gibco/BRL) and 0.1% bovine serum albumin (Sigma) in PBS and incubation with primary or secondary antibodies (36), coverslips were placed onto a solution of 1,4-diazabicyclo-[2.2.2]octane (25 mg/ml; Sigma) in Fluoromount-G (Southern Biotechnology Associates, Inc., Birmingham, Ala.). Images of fluorescence and phase contrast were collected with a 100× objective (oil immersion) as described above.

Establishment of vMIA-expressing and UL37x1 mutant-expressing cells. Sequences including UL37x1myc, UL37x1Δ115-130, or UL37x1Δ35-112/Δ148-163 were cloned into the expression vector pcDNALacHygro (Invitrogen) from the plasmids pcDNA3UL37x1myc, pcDNA3UL37x1Δ115-130, and UL37x1Δ35-112/Δ148-163 (20, 22), respectively, in place of the *lacZ* gene. To obtain pON2690, pcDNA3UL37x1myc was digested partially with *Bam*HI and to completion with *Xba*I and, following gel purification of the UL37x1myc fragment, was ligated to *Bam*HI- and *Xba*I-digested pcDNALacHygro. For clones pON2693 and pON2695, pcDNA3UL37x1Δ115-130 and UL37x1Δ35-112/Δ148-163, respectively, were digested with *Hin*dIII and *Xba*I and, following gel purification of the UL37x1 mutant fragment, were ligated to *Hin*dIII- and *Xba*I-digested pcDNALacHygro. All enzymes were obtained from New England Biolabs (Beverly, Mass.). The plasmids pON2690, pON2693, and pON2695 were used to isolate cells stably expressing vMIA or mutant proteins. Selection of G418-resistant, immortalized HF populations ihel.200 and ihel.400 followed retrovirus transduction with human papillomavirus type 18 E6 and E7 genes (21). After introduction of plasmids into the immortal cells, hygromycin was used to select vMIA.1 to vMIA.4 (from pON2690), UL37x1Δ115-130 (from pON2693), UL37x1Δ35-112/Δ148-163 (pON2695), or *lacZ*.1 through *lacZ*.3 from the parental vector.

Sedimentation of mitochondria. Primary HFs, vMIA.2 cells, and *lacZ*.1 cells were processed by standard differential sedimentation fractionation (39). In brief, cell monolayers were washed with PBS, scraped, and collected by centrifugation. The pellet was suspended in 0.5 ml of 10 mM NaCl, 1.5 mM $MgCl_2$, and 10 mM Tris-HCl (pH 7.5) and placed on ice for 10 min prior to disruption by Dounce homogenization before adding 0.8 ml of a solution containing 525 mM mannitol, 175 mM sucrose, 12.5 mM Tris-HCl (pH 7.5), and 2.5 mM EDTA. All buffers contained Complete protease inhibitors (Roche Molecular Biochemicals, Mannheim, Germany). The lysate was centrifuged at 4°C in a Tomy model TX-100 microcentrifuge through four rounds (1,000, 3,000, 3,000, and 15,000 × *g*). After each round pellets were suspended in sodium dodecyl sulfate-polyacrylamide gel electrophoresis disruption buffer, and equivalent cell fractions were separated by sodium dodecyl sulfate-polyacrylamide gel electrophoresis prior to transfer to nitrocellulose membranes and development by immunoblot analysis (39) using horseradish peroxidase-conjugated goat anti-mouse immunoglobulin G (Vector Laboratories) and the enhanced chemiluminescence system (Amersham, Piscataway, N.J.) according to the manufacturer's protocol.

Cell death assay. Cells were treated with medium containing anti-Fas antibody 7C11 at 0.2 μg/ml and CH at 10 μg/ml for 24 h as described previously (20) with the addition of trypan blue (Gibco/BRL) dye exclusion to the assay. For most experiments, parallel cultures were treated and returned to normal culture conditions prior to immunofluorescence detection of vMIA. For experiments using HeLa cells, immunofluorescence and propidium iodide staining was done immediately following Fas treatment.

Generation of BacvMIA. pON2696 was derived from an *Xba*I (filled)/*Nde*I vMIA-containing pcDNAUL37x1Myc fragment into *Nde*I- and *Sma*I-digested transfer vector MTS1 (48). pON2696 was transfected with BaculoGold (BD Biosciences, Franklin Lakes, N.J.) into Sf9 cells (11). A recombinant baculovirus capable of expressing US28-green fluorescent protein (US28-GFP) only in Sf9 cells was generated as a control. BacvMIA was used at a dose that gave 50% vMIA-positive HFs by immunofluorescence assay at 48 h postinfection (hpi). An equivalent volume of the control virus stock was used for comparison, and this represented 150 Sf9 cell infection units per HF. Protective activity of vMIA expressed from baculovirus was determined in HeLa cells at similar doses.

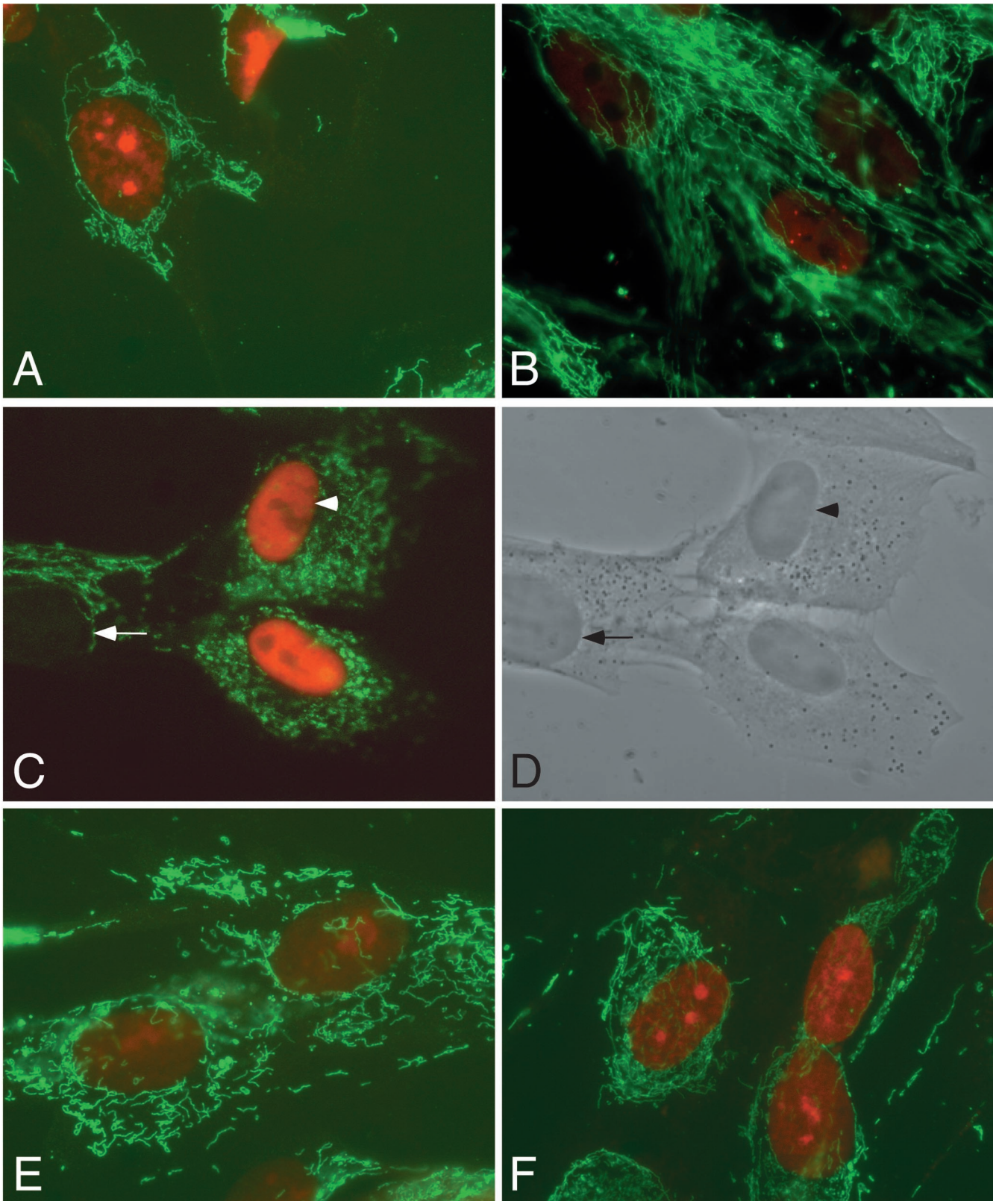

FIG. 1. Mitochondrial patterns within CMV-infected HFs. Cells were infected with human CMV strain AD169*var*ATCC for 8 or 24 h or 24 h in the presence of CH. Mitochondria were detected by antibodies to mtHSP70 (green). Nuclei were detected by antibodies to viral nuclear antigen (IE1/IE2) (red) (B and C) or by staining with propidium iodide (red) (A, E, and F). Mitochondria (green) and nuclei (red) are shown in uninfected HFs (A); uninfected HFs in the presence of CH for 24 h (F); or infected cells 8 (B) or 24 (C) hpi or at 24 hpi in the presence of CH (E). (D) Phase-contrast image of cells shown in panel C. The arrowhead indicates an infected cell, and the arrow indicates an uninfected cell.

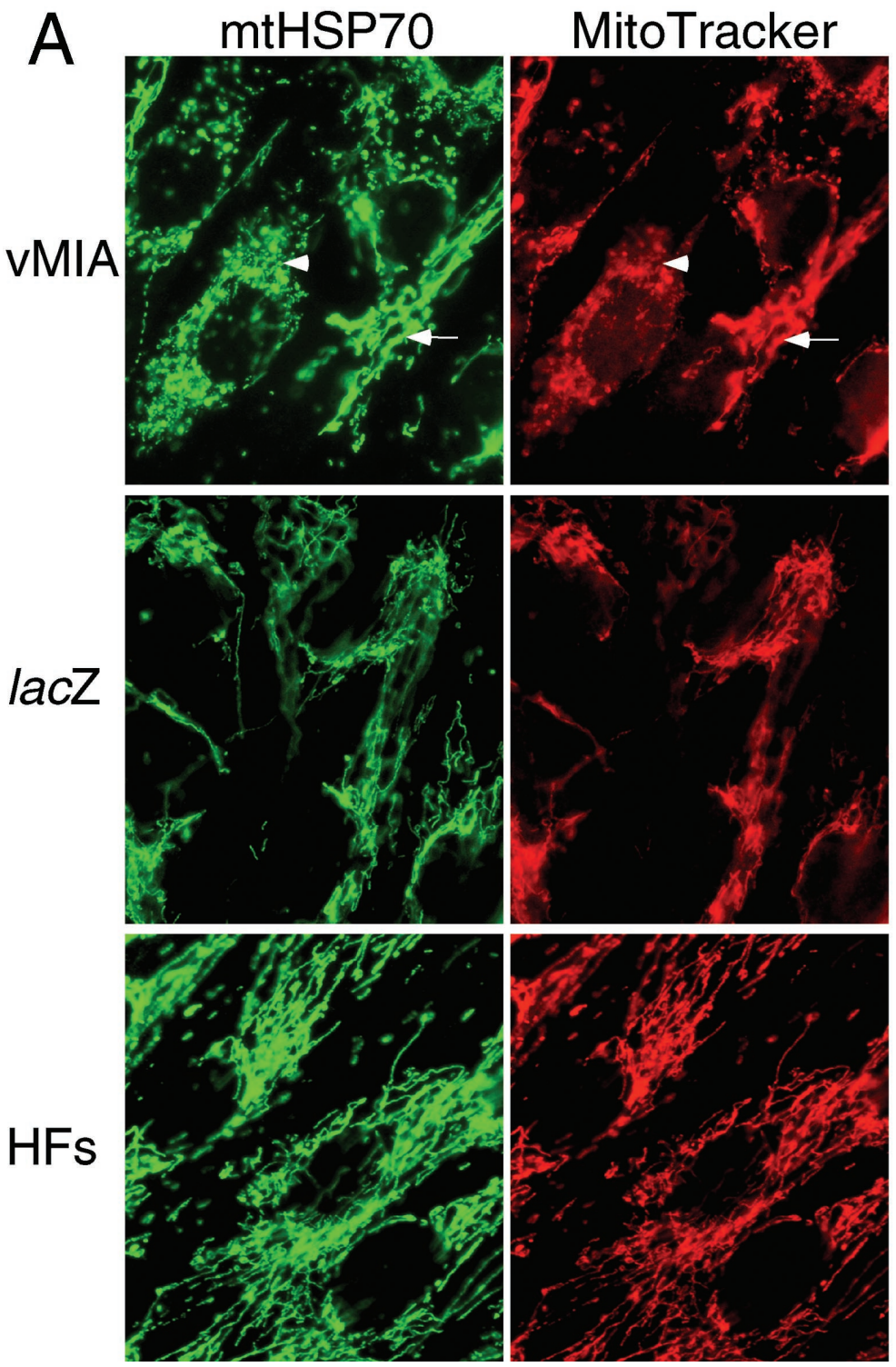

FIG. 2. Analysis of vMIA.2 cells. (A) Mitochondria detected by immunofluorescence (mtHSP70) in green (left column) and MitoTrackerRed in red (right column) in vMIA.2 (top row), *lacZ*.1 (middle row), and control HFs (bottom row). (B) MitoTrackerRed stain of mitochondria shown in red (image at left), immunofluorescence detection of vMIA shown in green (middle image), and overlay (image at right). (C) Examples of four patterns of vMIA-positive mitochondria visualized by immunofluorescence detection of vMIA. (D) Immunoblot analysis of mtHSP70 (top) and vMIA (bottom) following differential sedimentation fractionation of HFs, vMIA.2, and *lacZ*.1 cells. (E) vMIA-positive mitochondria (green) and propidium iodide-stained nuclei (red) in vMIA.2 cells (left) and in vMIA.2 cells following exposure to Fas-induction (right). (F) Immunoblot analysis of vMIA in CMV infection and vMIA.2 cells. Shown are mock- and CMV-infected HF lysates prepared at 24 or 72 h and vMIA.2 and *lacZ*.1 cell lysates collected before (vMIA.2, *lacZ*.1) or following exposure to anti-Fas antibody (vMIA.2+ and *lacZ*.1+). vMIA was detected using polyclonal antibody 313 to UL37x1 (top) or monoclonal antibody 9E10 to the myc epitope tag on vMIA.

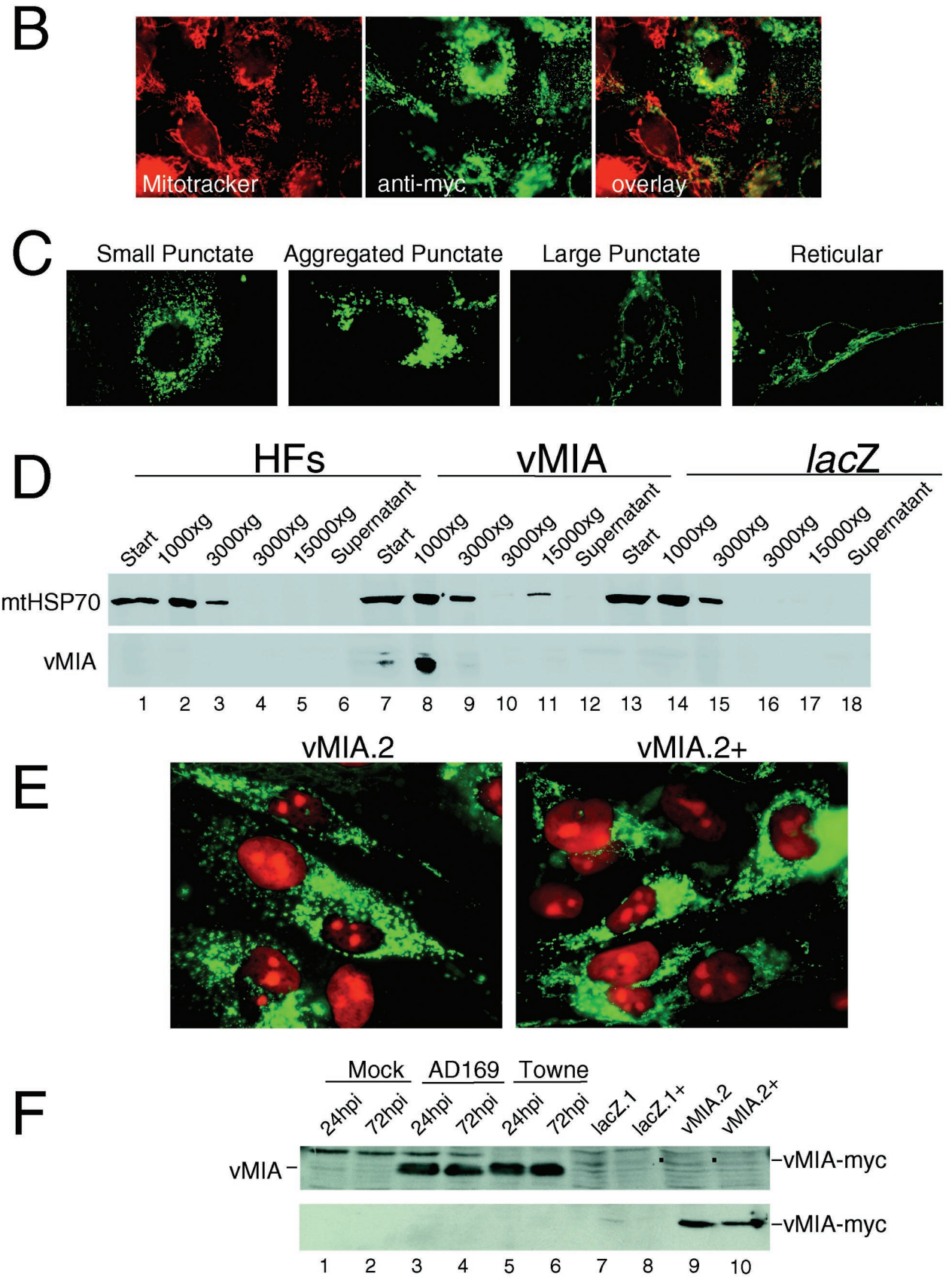

FIG. 2—*Continued*.

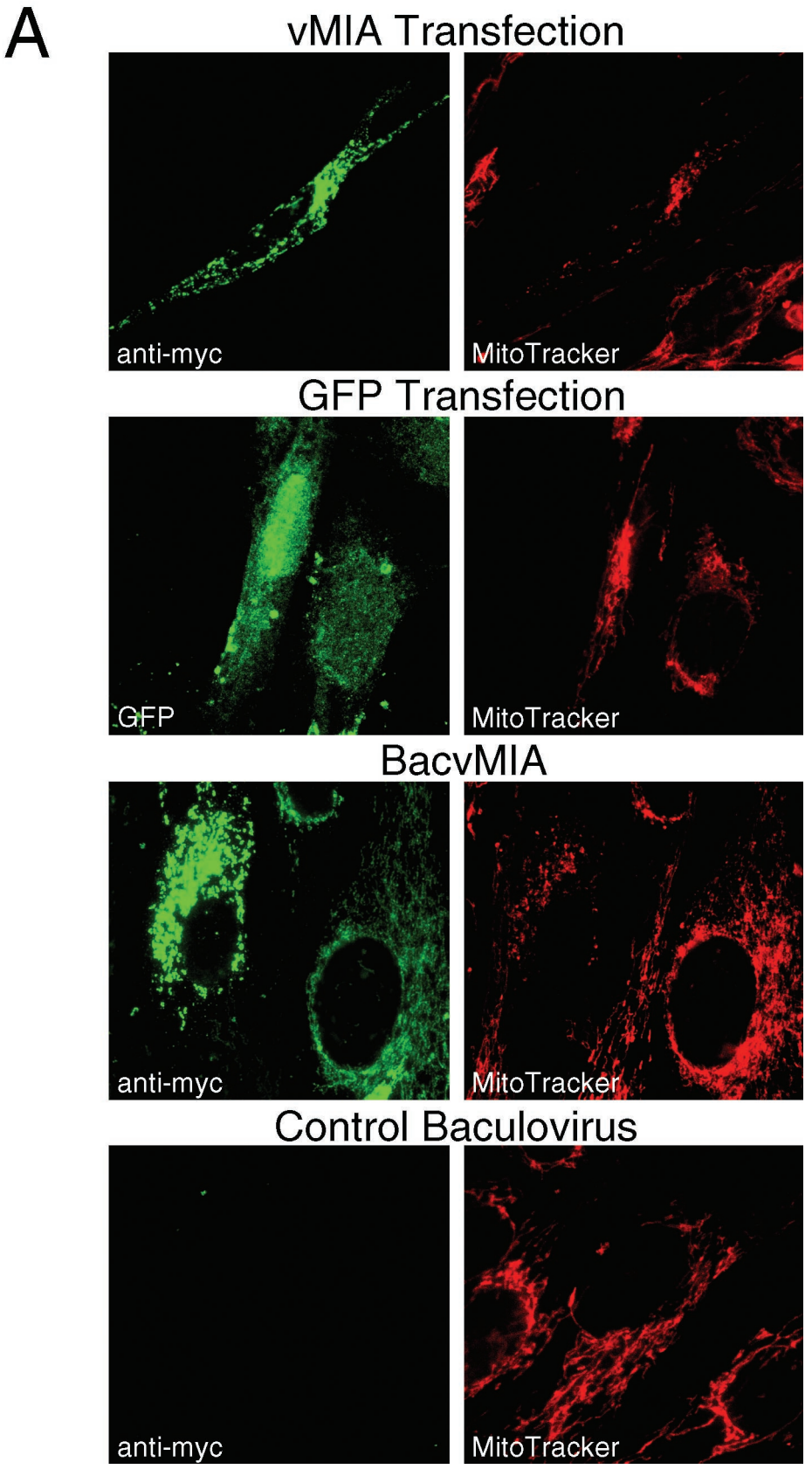
A
vMIA Transfection
anti-myc
MitoTracker
GFP Transfection
GFP
MitoTracker
BacvMIA
anti-myc
MitoTracker
Control Baculovirus
anti-myc
MitoTracker

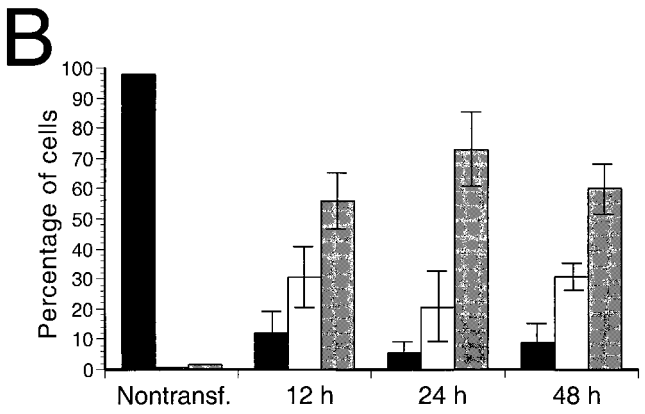

FIG. 3. Analysis of vMIA following transfection or transduction of HFs. (A) Mitochondrial morphology in cells following vMIA transfection or control GFP transfection (top four panels) and in cells transduced by BacvMIA or control baculovirus (bottom four panels). vMIA-positive cells were identified by anti-myc immunofluorescence detection, mitochondria were identified by MitoTrackerRed, and GFP-positive cells were identified by fluorescence as indicated on the panels. (B) Quantitation of cells expressing reticular, aggregated and/or large punctate, and small punctate mitochondria in control nontransfected cells (Nontransf.) and in cells transfected by vMIA expression plasmid at 12, 24, or 48 h. Nontransfected control cells were scored randomly, whereas only vMIA-positive cells were scored in transfected cells. Bars represent the means ± standard deviations (error bars) from three independent experiments. Black bars indicate reticular patterns, open bars indicate aggregated and large punctate patterns, and grey bars indicate small punctate patterns.

RESULTS

Mitochondrial organization during CMV infection. In order to assess changes that occur in mitochondrial organization following infection, human CMV (strain AD169*var*ATCC)-infected HFs (at 8, 24, or 48 hpi) were subjected to immunofluorescence analysis for the mitochondrion-resident protein mtHSP70 and for viral nuclear antigen IE1/IE2 (Fig. 1). Localization of mtHSP70 revealed the expected reticular network of mitochondria in uninfected HFs (Fig. 1A), and the network was evident through 8 hpi (Fig. 1B). By 24 hpi, however, mitochondria appeared punctate in cells that contained IE1/IE2 antigen (arrowhead in Fig. 1C and D). This disruption continued through late times of infection (data not shown) and occurred in virus-positive cells, but not in the virus-negative cells in the same cultures (arrow in Fig. 1C and D). Cells with a reticular staining pattern could not be distinguished from uninfected cells. A number of changes that have been observed to occur during CMV infection are induced by virus particle binding to the cell (7, 37). To determine whether de novo protein synthesis was required for mitochondrial disruption, cell cultures were infected and maintained in the presence of CH. CH-treated cells continued to exhibit a more reticular pattern (Fig. 1E). Mitochondrial networks in uninfected HFs were not altered by treatment with CH (Fig. 1F). Experiments carried out in parallel with MitoTrackerRed staining to monitor mitochondrial morphology gave similar patterns (data not shown), suggesting that mitochondrial disruption was apparent independent of the marker used. Combined, these data suggest that viral infection altered the mitochondrial networks normally associated with uninfected cells and implicate viral gene products made immediately following infection (α kinetic class) in this event. The only known viral α gene products that are targeted to mitochondria are encoded by *UL37*. Most experiments were carried out with CMV strain AD169*var*ATCC, which encodes three *UL37* gene products; however, infection with strain Towne*var*RIT3 also resulted in disruption of the reticular pattern (data not shown). Given that this Towne-based strain fails to express either of the larger UL37x1-containing proteins (gpUL37 or $gpUL37_M$), vMIA may be the cause of these alterations.

vMIA and mitochondrial organization. In order to assess the direct role of vMIA in mitochondrial disruption, we isolated HFs that stably express vMIA and compared mitochondrial morphology to control, β-galactosidase (β-Gal)-expressing cells. Initially, we localized mtHSP70 or MitoTrackerRed in cells that were identified as vMIA positive by virtue of a carboxyl-terminal c-myc epitope tag (20, 22). Using either marker, mitochondrial patterns ranged from reticular (arrow in Fig. 2A) to punctate (arrowhead in Fig. 2A) in the vMIA-expressing populations. Most control β-Gal-expressing or nontransformed parental HFs retained an expected reticular pattern (Fig. 2A). The proportion of vMIA-expressing cells exhibiting reticular or punctate staining patterns did not change with time up to 4 days postseeding, suggesting that the patterns formed independent of cell division or confluency. We next monitored the distribution of vMIA to determine whether localization patterns or intensity of vMIA staining correlated with the mitochondrial distribution (Fig. 2B). Maximal disruption of mitochondria was observed in cells with brightest staining for vMIA. vMIA was found in four distinct patterns: a small punctate pattern distributed throughout the cytoplasm; an aggregated punctate pattern with localization surrounding the nucleus; a large punctate pattern with what appeared to be fragmentation of networks; and an unaltered, reticular mitochondrial pattern (Fig. 2C). All vMIA-positive cells labeled with MitoTrackerRed, indicating that vMIA does not inhibit aerobic respiration; however, there was an inverse relationship of the intensity of the MitoTracker staining and the vMIA immunofluorescence signal. Reticular and large punctate patterns were brightest with MitoTrackerRed, whereas vMIA was brightest in the small punctate and aggregated punctate patterns. Alterations in mitochondrial morphology like these have not been previously reported for antiapoptotic viral proteins that target to mitochondria such as the Bcl homologs encoded by herpesviruses or adenoviruses. Patterns remarkably similar to these have been observed in COS-7 cells following induction of apoptosis and in cells that overexpress dynamin-related proteins that block apoptosis-induced mitochondrial fission (16, 29). Some of the vMIA-associated mitochondrial patterns may represent intermediates between the reticular and punctate patterns characterized in this work. The changes we observed may be due either to the ability of vMIA itself to induce mitochondrial fission or to a role for vMIA in stabilizing mitochondrial in these punctate forms by preventing fusion (see Discussion).

vMIA alteration of mitochondrial sedimentation properties. The disruption of mitochondria was further evaluated by cell fractionation. Cell lysates obtained from parental, vMIA-expressing, or β-Gal-expressing HFs were subjected to sequential sedimentation at 1,000, 3,000, and 15,000 × *g*, and material

that pelleted at each step was subjected to immunoblot analysis for mtHSP70 or vMIA (Fig. 2D). Based on this analysis, a majority of mitochondria sedimented at 1,000 and 3,000 × *g* in HFs or control β-Gal-expressing or vMIA-expressing cell lysates; however, mitochondria from vMIA-expressing cells were also found in the light mitochondrial fraction (15,000 × *g*). Analysis of starting material as well as the pellets that sedimented at 1,000 and 3,000 × *g* showed similar loading, and overall the results suggest that the sedimentation properties of mitochondria were altered in the presence of vMIA. The presence of light mitochondria was consistent with the smaller punctate staining observed in vMIA cells. mtHSP70 was not found in the supernatant of the 15,000 × *g* centrifugation, indicating that the small punctate immunofluorescent pattern was not due to complete lysis of mitochondria. vMIA was predominantly found in the cell fraction with the greatest mitochondria (from the centrifugation at 1,000 × *g*). Taken together with the MitoTracker staining, these results indicate that the small punctate staining pattern was due to a fission-like process and not due to the complete disruption of mitochondrial function or formation of nonfunctional mitochondrial remnants.

Localization of vMIA in cells that survive apoptosis. Although vMIA has been predicted to be important for virus infection, little characterization has been done in a relevant cell type like HFs (20, 22), although primary HFs have been shown to be resistant to Fas-mediated cell death following introduction of a vMIA-expression plasmid (19, 38). We compared the level of resistance among four vMIA-expressing HF populations (vMIA.1 to vMIA.4) and found the level of resistance to range from 29 to 54%, with vMIA.2 cells showing the greatest resistance. This population also had the highest percentage of vMIA-positive cells by immunofluorescence (43% positive). To determine whether the vMIA localization pattern changed following treatment with anti-Fas antibody, we compared untreated (vMIA.2 [Fig. 2E]) to treated cells (vMIA.2+ [Fig. 2E]). Although vMIA was present in vMIA.2 cells, the accumulation of vMIA was lower than that during virus infection. Immunoblot analysis using polyclonal anti-pUL37x1 antibody (a gift of Victor Goldmacher) revealed abundant vMIA accumulation in either AD169- or Towne-infected HFs at 24 or 72 hpi (Fig. 2F, lanes 3 to 6). Analysis of equivalent numbers of vMIA.2 cells either before or following Fas induction showed barely detectable levels using the anti-UL37x1 antibody but readily detectable levels with the anti-myc antibody (vMIA-myc) (Fig. 2F, lanes 9 and 10). The electrophoretic mobility of this protein in vMIA.2 cells was slower due to the presence of the epitope tag. As expected, β-Gal-positive, control cells collected before or after exposure to anti-Fas antibody did not contain vMIA (Fig. 2F, lanes 7 and 8). These results show that there is dramatically less vMIA in vMIA.2 cells compared to cells at 24 or 72 hpi but indicate that vMIA-mediated disruption of mitochondria occurs even at low expression levels.

Mitochondrial disruption in primary cells. In order to evaluate mitochondrial disruption in primary HFs, we introduced vMIA into cells by transfection of plasmid DNA or by transduction with a baculovirus-based mammalian expression vector (11). Mitochondria were disrupted and appeared punctate within 12 h when vMIA was delivered by either method (Fig. 3A). Cells that remained vMIA negative as well as cells that had been transfected with a control plasmid or transduced by a control baculovirus retained a reticular pattern. Cells expressing vMIA exhibited one of the four patterns observed in stable vMIA-expressing HFs (Fig. 2C). When aggregated punctate and large punctate patterns were scored together as a single class, the proportion of cells in each of the three resulting classes did not change over time (Fig. 3B). Thus, disruption in primary cells occurs rapidly and is maintained over a period when vMIA has been shown to protect from apoptosis (19, 38).

Minimal vMIA domains for disruption. To determine whether the previously identified vMIA mitochondrial localization and antiapoptotic domains were critical for disruption of mitochondria, myc-tagged mutants of vMIA were used to derive stable ihel.200 cells (Fig. 4). Cell lines allowed evaluation of vMIA localization over many cell doublings and in cells with different mitochondrial patterns. Cells with the 68-amino-acid fully functional mutant UL37x1Δ35-112/Δ148-163 (22) exhibited the full range of small punctate, aggregated punctate, large punctate, and reticular patterns comparable to the full-length protein. A majority of cells exhibited one of the three punctate patterns. As was the case for the full-length protein, mitochondrial networks stained less intensely for vMIA and more intensely for MitoTracker than punctate mitochondria (compare cells marked with arrow and arrowhead, respectively, in Fig. 4A and B). This result suggests that mitochondrial disruption is a property of the minimal, but fully protective vMIA construct. This result also suggests that disruption appeared independent of protein size, with vMIA, at 163 amino acids, and UL37x1Δ35-112/Δ148-163, at 68 amino acids, showing similar patterns. UL37x1Δ115-130, a mitochondrion-localized mutant that fails to block apoptosis (22), was employed to determine whether the ability to localize but not protect from apoptosis was sufficient to cause a conversion to a punctate staining pattern. In two independent UL37x1Δ115-130-positive cell populations, the majority of cells retained a reticular pattern (Fig. 4C and D), although a small percentage of punctate cells were present (data not shown). In contrast to the situation with full-length vMIA or with UL37x1Δ35-112/Δ148-163, the UL37x1Δ115-130-positive cells with a reticular pattern were no less bright than the few cells with a punctate pattern (data not shown). These results suggest that targeting to mitochondria was insufficient to disrupt reticular patterns. These results also establish a correlation between the ability of vMIA to disrupt mitochondrial networks and the established antiapoptotic behavior of vMIA (20, 22).

DISCUSSION

Evidence suggests that *UL37x1* is important for CMV infection by encoding the potent antiapoptotic function, vMIA (19). Although *UL37x1* also encodes the amino terminus of two larger *UL37* gene products (gpUL37 and gpUL37$_M$), these are dispensable for replication in HFs (4, 20) and have a carboxyl terminus that may confer additional functions (23). vMIA plays a role in apoptosis by associating with mitochondrial megapore component ANT (19, 43) and is broadly active against a wide range of inducers (3, 24, 43). The lack of amino acid sequence similarity as well as the failure to exhibit an interaction with the voltage-dependent anion channel distin-

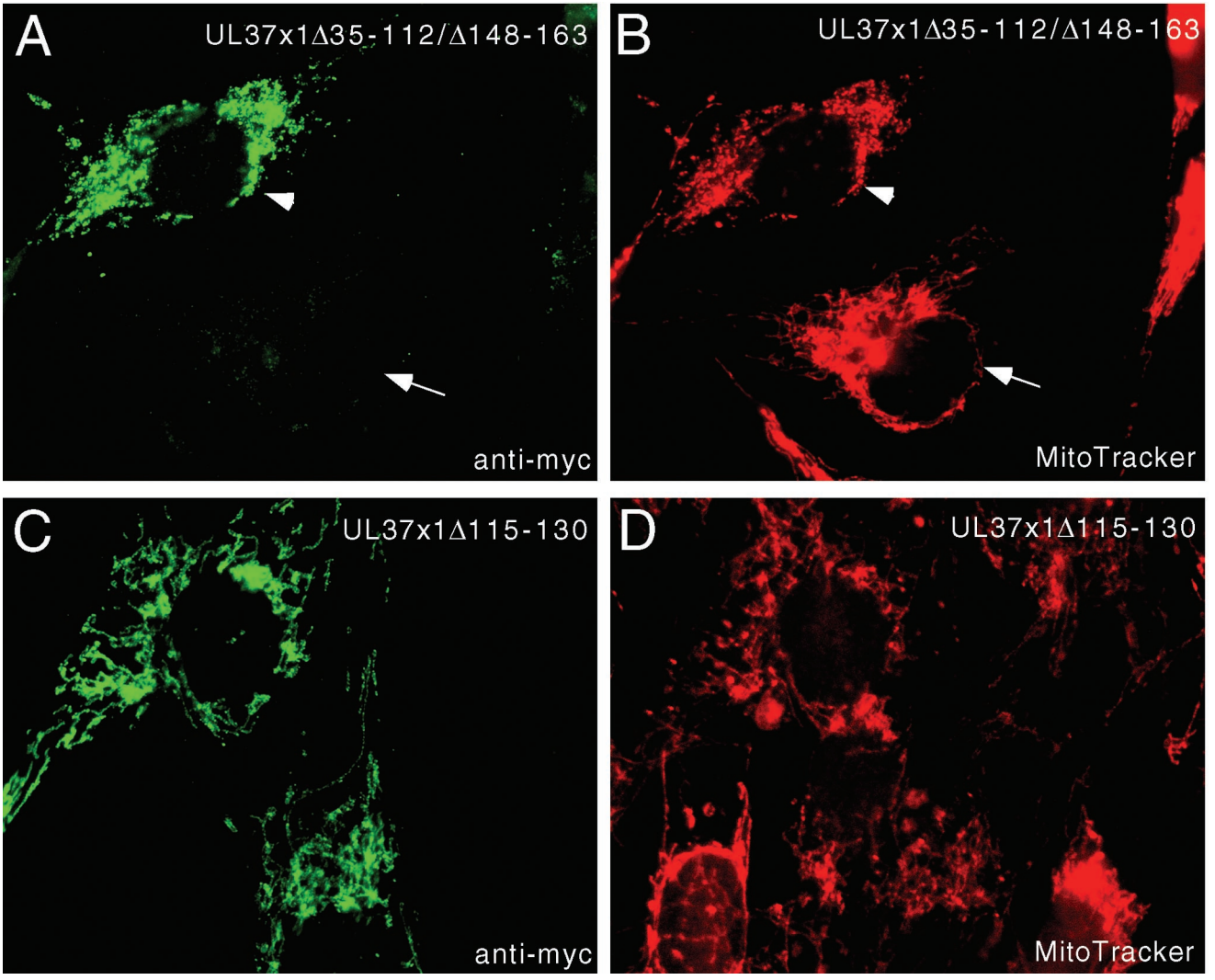

FIG. 4. Mitochondrial morphology in cells expressing vMIA mutants. Stable UL37x1Δ35-112/Δ148-163 (A and B)- or UL37x1Δ115-130 (C and D)-expressing cells were analyzed for mitochondrial morphology. Immunofluorescence detection of UL37x1 mutants is shown in green (left panels), and MitoTrackerRed staining is shown in red (right panels).

guishes vMIA from the large number of antiapoptotic Bcl family members encoded by herpesviruses, adenoviruses, and their mammalian hosts (5, 19). Here we have shown that vMIA disrupts mitochondria, possibly by inducing fission or preventing fusion, and this is associated with an ability to block apoptosis. Induction of fission has previously been associated with signals that trigger apoptosis. A dominant-negative mutant of the mitochondrial fission protein dynamin-related protein 1 has been employed to suggest that inhibition of fission blocks apoptosis (16). vMIA seems uniquely able to induce a similar type of change without itself being proapoptotic. Furthermore, the level to which mitochondrial disruption occurs in vMIA-expressing cells appears independent of death receptor signaling.

We have observed disruption of mitochondria during CMV infection in a pattern similar to that induced by vMIA alone. Mitochondrial networks are certainly disrupted by stress such as heat shock (9) and herpesvirus infection (31, 34). During the first 24 h following CMV infection, vMIA accumulation correlated with mitochondrial disruption. Disruption of mitochondria was prevented by inhibition of protein synthesis, suggesting the direct involvement of vMIA in disruption of mitochondrial networks. An alternative explanation, that vMIA altered recovery from a stress response induced by viral infection, remains a possibility. Following heat shock, mitochondria accumulate around the nucleus within 1 h but regain a reticular organization within 24 h (9). The mitochondria in CMV-infected cells did not regain a reticular pattern at any time examined, consistent with the continued role of vMIA in maintaining disruption as cells become resistant to apoptosis (20).

During cell growth, the processes of mitochondrial fission and fusion regulate the morphology of mitochondrial networks within the cell. The recent report from Frank et al. (16) suggests the importance of mitochondrial fission during apoptosis. MitoTrackerRed staining has been widely used to assess changes in respiration, including work that correlated fission with depolarization during apoptosis. We used this reagent to

show that vMIA-mediated disruption of mitochondria does not depolarize, consistent with full mitochondrial activity continuing during CMV replication. We suspect that the process we have observed is due to increased rates of fission or decreased rates of fusion rather than to other processes known to alter mitochondria. Perturbations such as damage to mitochondria that alter the rate of mitochondrial turnover and lead to autophagy, prevent attachment of mitochondria to the cytoskeleton, or result in a loss of mitochondrial DNA are not as consistent with the phenotype we observed in stable vMIA-positive cells. The process of autophagy results in the complete loss of mitochondria within days (42) due to increased degradation (25), which is preceded by perinuclear clustering (42) and loss of membrane potential (15). In contrast, vMIA-positive mitochondria continue to respire, and vMIA-positive cells continue to grow and divide. Mutations altering kinesins lead to clustering of mitochondria around the nucleus (41). Although clustering occurs in some vMIA-positive cells, others exhibit nonclustered micropunctate mitochondria, suggesting a function independent of kinesins and microtubules. Finally, mitochondrial DNA depletion leads to a loss in respiration and reticular networks (18). Although vMIA-positive mitochondria are not reticular, they retain the ability to accumulate MitoTrackerRed consistent with active respiration and maintenance of mitochondrial DNA. In summary, data from stable vMIA-positive cells provide the best evidence that fission and/or fusion events are altered by vMIA. The changes we observed may be due to the ability of vMIA itself to either increase rates of mitochondrial fission or decrease rates of fusion. Whether these changes occur solely as a result of vMIA-ANT interactions remains to be determined.

Mitochondrion-targeted inhibitors of adenovirus have been well-characterized and illustrate virus-mediated inhibition of intrinsic apoptosis. Adenovirus E1B blocks apoptosis by preventing Bax and Bak function (12). Bax is a cytoplasmic protein that translocates to the mitochondria and undergoes a conformational change during apoptosis. Bax also interacts with a specific conformation of ANT to form channels with unique electrophysiological properties that have been suggested to mediate mitochondrial permeability transition (6). Bax resides briefly in mitochondria prior to accumulating with Bak in clusters outside of this organelle (33). At some point, Bax also disrupts mitochondrial networks (16). Direct interaction of E1B with Bak, a mitochondrial protein, does not allow Bak to interact with Bax, so that Bax remains nonfunctional (12). Although vMIA has not been shown to bind Bak or any other proapoptotic Bcl family members directly, it may have similar effects. First the vMIA-ANT interaction may alter proapoptotic function of Bax. It is possible that vMIA, by interaction with ANT, prevents Bax-ANT channel formation without altering ATP/ADP exchange. Regulation of proapoptotic proteins may occur at other levels as well. Thus, vMIA may interfere with apoptosis by inhibiting one of the steps leading to activation of Bax perhaps through premature fission of mitochondria.

ACKNOWLEDGMENTS

This work was supported by PHS grant RO1 AI20211 (to E.S.M.) and NRSA grant F32 AI09855 (to A.L.M.).

We thank Laura Hertel and Geoff Smith for critical reading of the manuscript.

REFERENCES

1. **Abbate, J., J. C. Lacayo, M. Prichard, G. Pari, and M. A. McVoy.** 2001. Bifunctional protein conferring enhanced green fluorescence and puromycin resistance. BioTechniques **31:**336–340.
2. **Barber, G. N.** 2001. Host defense, viruses and apoptosis. Cell Death Differ. **8:**113–126.
3. **Belzacq, A. S., C. El Hamel, H. L. Vieira, I. Cohen, D. Haouzi, D. Metivier, P. Marchetti, C. Brenner, and G. Kroemer.** 2001. Adenine nucleotide translocator mediates the mitochondrial membrane permeabilization induced by lonidamine, arsenite and CD437. Oncogene **20:**7579–7587.
4. **Borst, E. M., G. Hahn, U. H. Koszinowski, and M. Messerle.** 1999. Cloning of the human cytomegalovirus (HCMV) genome as an infectious bacterial artificial chromosome in *Escherichia coli*: a new approach for construction of HCMV mutants. J. Virol. **73:**8320–8329.
5. **Boya, P., B. Roques, and G. Kroemer.** 2001. New EMBO members' review: viral and bacterial proteins regulating apoptosis at the mitochondrial level. EMBO J. **20:**4325–4331.
6. **Brenner, C., H. Cadiou, H. L. Vieira, N. Zamzami, I. Marzo, Z. Xie, B. Leber, D. Andrews, H. Duclohier, J. C. Reed, and G. Kroemer.** 2000. Bcl-2 and Bax regulate the channel activity of the mitochondrial adenine nucleotide translocator. Oncogene **19:**329–336.
7. **Browne, E. P., B. Wing, D. Coleman, and T. Shenk.** 2001. Altered cellular mRNA levels in human cytomegalovirus-infected fibroblasts: viral block to the accumulation of antiviral mRNAs. J. Virol. **75:**12319–12330.
8. **Colberg-Poley, A. M., M. B. Patel, D. P. Erezo, and J. E. Slater.** 2000. Human cytomegalovirus UL37 immediate-early regulatory proteins traffic through the secretory apparatus and to mitochondria. J. Gen. Virol. **81:**1779–1789.
9. **Collier, N. C., M. P. Sheetz, and M. J. Schlesinger.** 1993. Concomitant changes in mitochondria and intermediate filaments during heat shock and recovery of chicken embryo fibroblasts. J. Cell Biochem. **52:**297–307.
10. **Collins, T. J., M. J. Berridge, P. Lipp, and M. D. Bootman.** 2002. Mitochondria are morphologically and functionally heterogeneous within cells. EMBO J. **21:**1616–1627.
11. **Condreay, J. P., S. M. Witherspoon, W. C. Clay, and T. A. Kost.** 1999. Transient and stable gene expression in mammalian cells transduced with a recombinant baculovirus vector. Proc. Natl. Acad. Sci. USA **96:**127–132.
12. **Cuconati, A., K. Degenhardt, R. Sundararajan, A. Anschel, and E. White.** 2002. Bak and Bax function to limit adenovirus replication through apoptosis induction. J. Virol. **76:**4547–4558.
13. **De Vos, K., V. Goossens, E. Boone, D. Vercammen, K. Vancompernolle, P. Vandenabeele, G. Haegeman, W. Fiers, and J. Grooten.** 1998. The 55-kDa tumor necrosis factor receptor induces clustering of mitochondria through its membrane-proximal region. J. Biol. Chem. **273:**9673–9680.
14. **Edwards, K. M., J. E. Davis, K. A. Browne, V. R. Sutton, and J. A. Trapani.** 1999. Anti-viral strategies of cytotoxic T lymphocytes are manifested through a variety of granule-bound pathways of apoptosis induction. Immunol. Cell Biol. **77:**76–89.
15. **Elmore, S. P., T. Qian, S. F. Grissom, and J. J. Lemasters.** 2001. The mitochondrial permeability transition initiates autophagy in rat hepatocytes. FASEB J. **15:**2286–2287.
16. **Frank, S., B. Gaume, E. S. Bergmann-Leitner, W. W. Leitner, E. G. Robert, F. Catez, C. L. Smith, and R. J. Youle.** 2001. The role of dynamin-related protein 1, a mediator of mitochondrial fission, in apoptosis. Dev. Cell **1:**515–525.
17. **Furukawa, T., S. Sakuma, and S. A. Plotkin.** 1976. Human cytomegalovirus infection of WI-38 cells stimulates mitochondrial DNA synthesis. Nature **262:**414–416.
18. **Gilkerson, R. W., D. H. Margineantu, R. A. Capaldi, and J. M. Selker.** 2000. Mitochondrial DNA depletion causes morphological changes in the mitochondrial reticulum of cultured human cells. FEBS Lett. **474:**1–4.
19. **Goldmacher, V. S.** 2002. vMIA, a viral inhibitor of apoptosis targeting mitochondria. Biochimie **84:**177–185.
20. **Goldmacher, V. S., L. M. Bartle, A. Skaletskaya, C. A. Dionne, N. L. Kedersha, C. A. Vater, J. Han, R. J. Lutz, S. Watanabe, E. D. McFarland, E. D. Kieff, E. S. Mocarski, and T. Chittenden.** 1999. A cytomegalovirus-encoded mitochondria-localized inhibitor of apoptosis structurally unrelated to Bcl-2. Proc. Natl. Acad. Sci. USA **96:**12536–12541.
21. **Greaves, R. F., J. M. Brown, J. Vieira, and E. S. Mocarski.** 1995. Selectable insertion and deletion mutagenesis of the human cytomegalovirus genome using the *Escherichia coli* guanosine phosphoribosyl transferase (gpt) gene. J. Gen. Virol. **76:**2151–2160.
22. **Hayajneh, W. A., A. M. Colberg-Poley, A. Skaletskaya, L. M. Bartle, M. M. Lesperance, D. G. Contopoulos-Ioannidis, N. L. Kedersha, and V. S. Goldmacher.** 2001. The sequence and antiapoptotic functional domains of the human cytomegalovirus UL37 exon 1 immediate early protein are conserved in multiple primary strains. Virology **279:**233–240.
23. **Hayajneh, W. A., D. G. Contopoulos-Ioannidis, M. M. Lesperance, A. M. Venegas, and A. M. Colberg-Poley.** 2001. The carboxyl terminus of the human cytomegalovirus UL37 immediate-early glycoprotein is conserved in

primary strains and is important for transactivation. J. Gen. Virol. **82:**1569–1579.
24. **Jan, G., A. S. Belzacq, D. Haouzi, A. Rouault, D. Metivier, G. Kroemer, and C. Brenner.** 2002. Propionibacteria induce apoptosis of colorectal carcinoma cells via short-chain fatty acids acting on mitochondria. Cell Death Differ. **9:**179–188.
25. **Klionsky, D. J., and S. D. Emr.** 2000. Autophagy as a regulated pathway of cellular degradation. Science **290:**1717–1721.
26. **Landini, M. P., and M. Rugolo.** 1984. Increased accumulation of a lipophilic cation (tetraphenylphosphonium) in human embryo fibroblasts after infection with cytomegalovirus. J. Gen. Virol. **65:**2269–2272.
27. **Li, H., H. Zhu, C. J. Xu, and J. Yuan.** 1998. Cleavage of BID by caspase 8 mediates the mitochondrial damage in the Fas pathway of apoptosis. Cell **94:**491–501.
28. **Lu, M., and T. Shenk.** 1999. Human cytomegalovirus UL69 protein induces cells to accumulate in G_1 phase of the cell cycle. J. Virol. **73:**676–683.
29. **Misaka, T., T. Miyashita, and Y. Kubo.** 2002. Primary structure of a dynamin-related mouse mitochondrial GTPase and its distribution in brain, subcellular localization, and effect on mitochondrial morphology. J. Biol. Chem. **277:** 15834–15842.
30. **Mocarski, E. S., Jr., and C. T. Courcelle.** 2001. Cytomegaloviruses and their replication., p. 2629–2673. *In* D. M. Knipe, P. M. Howley, D. E. Griffin, et al. (ed.), Fields virology. Lippincott Williams & Wilkins, Philadelphia, Pa.
31. **Murata, T., F. Goshima, T. Daikoku, K. Inagaki-Ohara, H. Takakuwa, K. Kato, and Y. Nishiyama.** 2000. Mitochondrial distribution and function in herpes simplex virus-infected cells. J. Gen. Virol. **81:**401–406.
32. **Murphy, E. A., D. N. Streblow, J. A. Nelson, and M. F. Stinski.** 2000. The human cytomegalovirus IE86 protein can block cell cycle progression after inducing transition into the S phase of permissive cells. J. Virol. **74:**7108–7118.
33. **Nechushtan, A., C. L. Smith, I. Lamensdorf, S. H. Yoon, and R. J. Youle.** 2001. Bax and Bak coalesce into novel mitochondria-associated clusters during apoptosis. J. Cell Biol. **153:**1265–1276.
34. **Nishiyama, Y., and T. Murata.** 2002. Anti-apoptotic protein kinase of herpes simplex virus. Trends Microbiol. **10:**105–107.
35. **Patterson, C. E., and T. Shenk.** 1999. Human cytomegalovirus UL36 protein is dispensable for viral replication in cultured cells. J. Virol. **73:**7126–7131.
36. **Penfold, M. E., and E. S. Mocarski.** 1997. Formation of cytomegalovirus DNA replication compartments defined by localization of viral proteins and DNA synthesis. Virology **239:**46–61.
37. **Simmen, K. A., J. Singh, B. G. Luukkonen, M. Lopper, A. Bittner, N. E. Miller, M. R. Jackson, T. Compton, and K. Fruh.** 2001. Global modulation of cellular transcription by human cytomegalovirus is initiated by viral glycoprotein B. Proc. Natl. Acad. Sci. USA **98:**7140–7145.
38. **Skaletskaya, A., L. M. Bartle, T. Chittenden, A. L. McCormick, E. S. Mocarski, and V. S. Goldmacher.** 2001. A cytomegalovirus-encoded inhibitor of apoptosis that suppresses caspase-8 activation. Proc. Natl. Acad. Sci. USA **98:**7829–7834.
39. **Spector, D., R. Goldman, and L. Leinwand (ed.).** 1998. Cells: a laboratory manual. Cold Spring Harbor Laboratory Press, Cold Spring Harbor, N.Y.
40. **Tanaka, K., J. P. Zou, K. Takeda, V. J. Ferrans, G. R. Sandford, T. M. Johnson, T. Finkel, and S. E. Epstein.** 1999. Effects of human cytomegalovirus immediate-early proteins on p53-mediated apoptosis in coronary artery smooth muscle cells. Circulation **99:**1656–1659.
41. **Tanaka, Y., Y. Kanai, Y. Okada, S. Nonaka, S. Takeda, A. Harada, and N. Hirokawa.** 1998. Targeted disruption of mouse conventional kinesin heavy chain, kif5B, results in abnormal perinuclear clustering of mitochondria. Cell **93:**1147–1158.
42. **Tolkovsky, A. M., L. Xue, G. C. Fletcher, and V. Borutaite.** 2002. Mitochondrial disappearance from cells: a clue to the role of autophagy in programmed cell death and disease? Biochimie **84:**233–240.
43. **Vieira, H. L., A. S. Belzacq, D. Haouzi, F. Bernassola, I. Cohen, E. Jacotot, K. F. Ferri, C. El Hamel, L. M. Bartle, G. Melino, C. Brenner, V. Goldmacher, and G. Kroemer.** 2001. The adenine nucleotide translocator: a target of nitric oxide, peroxynitrite, and 4-hydroxynonenal. Oncogene **20:**4305–4316.
44. **Wallach, D., E. E. Varfolomeev, N. L. Malinin, Y. V. Goltsev, A. V. Kovalenko, and M. P. Boldin.** 1999. Tumor necrosis factor receptor and Fas signaling mechanisms. Annu. Rev. Immunol. **17:**331–367.
45. **White, E.** 2001. Regulation of the cell cycle and apoptosis by the oncogenes of adenovirus. Oncogene **20:**7836–7846.
46. **Yaffe, M. P.** 1999. The machinery of mitochondrial inheritance and behavior. Science **283:**1493–1497.
47. **Yu, Y., and J. C. Alwine.** 2002. Human cytomegalovirus major immediate-early proteins and simian virus 40 large T antigen can inhibit apoptosis through activation of the phosphatidylinositide 3′-OH kinase pathway and the cellular kinase Akt. J. Virol. **76:**3731–3738.
48. **Zhou, G., V. Galvan, G. Campadelli-Fiume, and B. Roizman.** 2000. Glycoprotein D or J delivered in *trans* blocks apoptosis in SK-N-SH cells induced by a herpes simplex virus 1 mutant lacking intact genes expressing both glycoproteins. J. Virol. **74:**11782–11791.
49. **Zhu, H., Y. Shen, and T. Shenk.** 1995. Human cytomegalovirus IE1 and IE2 proteins block apoptosis. J. Virol. **69:**7960–7970.